Silicon (2019) 11:2675–2688
https://doi.org/10.1007/s12633-018-0056-1

ORIGINAL PAPER

Vitrified Municipal Waste for the Immobilization of Radioactive Waste: Preparation and Characterization of Borosilicate Glasses Modified with Metal Oxides

E. M. Abou Hussein [1]

Received: 10 October 2018 / Accepted: 10 December 2018 / Published online: 2 January 2019

Abstract
Municipal solid waste is used as a raw material for the production of borosilicate glasses by melting annealing technique. Many chemical and physical measurements are studied to test their possibility in the immobilization of radioactive wastes. The results show good behaviors against gamma radiation doses such as suitable density and microhardness values, stable behaviors towards low and high doses of gamma radiation indicated by IR and EPR techniques. As well as good chemical durability in H_2O and NaOH leaching solutions. The network structure of borosilicate glasses consists of tetrahedral silicate units SiO_4 and the triangle BO_3 or tetrahedral BO_4 groups which strengthen the structure of glasses and enhance their desired properties for achieving the goal of immobilizing nuclear wastes.

Keywords Vitrification · Nuclear waste glass · Gamma radiation · Borosilicate · Chemical durability

1 Introduction

Many tremendous dangers and environmental problems are caused by the accumulation of municipal solid wastes (MSWs). Therefore management of MSWs becomes with urgent necessity. Recycling of wastes is a good solution but only about 40% of their total volume can be recycled. The Landfilling process is commonly used in developing countries where the incineration process is used in the European countries in order to reduce weight and volume of wastes and recover energy [1]. However the ash residues lagging behind them cause another environmental problem [2]. Therefore using theses accumulative ash residues in cement industry or in the vitrification process is a useful commercial solution. In vitrification process, the ashes are used as raw materials in the production of applicable commercial glasses or glass ceramics [3, 4]. The waste vitrification is the process to select a glass matrix has the ability to incorporate the radioactive wastes according to the flexibility of the glasses and their disordered structures [5].

Vitrification needs high costs due to energy consumption, but this problem can be overcome by two ways; (1) the addition of a specific chemical material that enhances the process by decreasing the temperature required for melting, such as soda (Na_2O), or potash (K_2O) where their additions to silica can lower the softening point by 800–900 °C [6]. (2) The production of high valuable products to help in offsetting the cost like nuclear waste glasses [7]. Nuclear waste glass is one of the most useful applications of the MSWs vitrification, because it can be used as a safe and long range hosting matrix for the immobilization of hazardous radioactive wastes and heavy metals. Borosilicate glasses are the most common nuclear waste glasses that are previously prepared like SON68, WAK and Pamela [8]. They are accepted to be the first generation waste form for the immobilization of high level radioactive wastes HLW [9]. Borosilicate glasses consist of a complex glassy network from the glass forming oxides; SiO_2 and B_2O_3. Their complicated structure enable them to be the first candidate for immobilizing the high level radioactive wastes HLW because of their flexibility to incorporate many types of waste elements through the highly atomic bonding between them and the glassy network [9–11]. Borosilicate glasses have also high chemical durability, mechanical reliability,

✉ E. M. Abou Hussein
Eman_muhammed@yahoo.com

[1] Radiation Chemistry Department, National Center for Radiation Research and Technology, Atomic Energy Authority, P. O. Box 8029, Nasr City, Cairo 11371, Egypt

remarkable thermal and radiation stability as well as high chemical resistance in most leaching media.

The Presence of a specific metal oxide can enhance the properties of borosilicate glasses for immobilizing radioactive wastes; for example Al^{3+} ions participate in the glass network as AlO_4 and/or AlO_6 structural units [12] and give the glasses high radiation resistance capability because of forming strong covalent bonds including SiO_4, BO_4 and AlO_4 tetrahedral units. Ca^{2+} ions can enhance also some of their mechanical and chemical properties such as microhardness and chemical durability. Miae Kim and Jong Heo [13] have investigated that the waste forms of calcium-borosilicate glass-ceramics can be used for the immobilization of rare-earth oxide wastes from pyro-processing. Fe^{3+} ions also provide the radiation shielding effect of the glass that introduced in, because of its two oxidation states 4 and 6 and their tendency to form strong coordinations from tetrahedral and/ or octahedral units [14].

The general effect of ionizing radiation on glasses is the formation of induced defect centers and non- bridging hole centers as shown in the following radiation chemical reaction [7].

$$(\equiv Si–O–M)\ \text{glass} + \gamma\ \text{irradiation} \rightarrow \equiv Si–O^{\bullet} + M^{+} \quad (1)$$

Specifically, the influence of radiation on borosilicate glasses is more complicated than the vitreous silicate glasses because of the cooperation between the two main phase natures of SiO_2 and B_2O_3 that provide their ability to shield radiation. Although, Nuclear wastes become less radioactive the longer they are stored because of their radioactive decay, some of their radioactivity continues for millions of years [15]. Gamma radiations are emitted in the nuclear waste glass during the first hundreds of years [16] so the bezel efficiency of nuclear waste glasses is measured by their tendency to resist the effect of gamma radiations and preventing their passages.

The aim of the present work is to prepare three compositions of CaO, Al_2O_3 and Fe_2O_3 sodium borosilicate glasses by using burned MSWs as a raw material. In addition to, studying the possibility of using them as nuclear waste glasses by making a comparative study between some of their physical and chemical properties at different doses of gamma radiation. Density, microhardness, Infrared absorption spectra FTIR, electron paramagnetic resonance EPR and chemical durability; all of these measurements are studied to verify the desired goal in using these compositions as nuclear waste glasses.

2 Experimental Procedure

Glasses were prepared by the conventional melt-quench annealing technique. In accordance with their compositions tabulated in Table 1, homogenous mixtures of batches were prepared and accurately weighed. The raw materials used in preparation were; MSW taken from a waste collecting region in eastern Cairo zone at Khatamia, and burned at 700 °C. Also pure grade reagents from H_3BO_3, SiO_2, Na_2CO_3, $CaCO_3$, Al_2O_3 and Fe_2O_3 from Sigma-Aldrich Company were used in preparation. By using a gate mortar, the accurately weighed chemical compounds of each glass composition were mixed thoroughly to fine powders. Then melted in a porcelain crucible in an electric furnace at 1200–1300 °C for 3 h with rotating melts to attain homogeneity and remove air bubbles. The melts were then cast into preheated stainless steel hot molds with dimensions of 1x1x0.2 cm^3 and the prepared samples were immediately moved to a muffle furnace regulated at 500 °C for annealing. After 1 h, the muffle was switched off and samples were left overnight where the muffle temperature decreased to room temperature with a cooling rate ±25 °C /h. The chemical analysis of each glass sample was detected by using electron dispersive X- ray analyzer EDX and the data were listed in Table 2.

Table 1 Chemical compositions of the prepared glasses in wt.%

Glass no.	Waste	B_2O_3	SiO_2	Na_2O	CaO	Al_2O_3	Fe_2O_3
G1	50	20	10	15	5		
G2	50	20	10	15		5	
G3	50	20	10	15			5

In order to assure the amorphous structural natures of the prepared glasses, X-ray diffraction patterns of the samples were detected by using a Shimadzu XD-DI diffractometer. The X-ray was operated at 40 kV and 30 mA through the measurements at the room temperature and under constant operating conditions.

Testing chemical durability of the prepared glasses was carried out by three leaching experiments a, b and c. (a) at 90 °C for 16 h (b) At different irradiation doses from 10 to 200 kGy, where the leaching solution in (a) and (b) was underground water taken from a deep well in the Egyptian Siwa oasis with a chemical composition of 5.2 Ca, 17.0 K, 37 Na, 95.16 bicarbonates, 14 sulphates, 33 chlorides, 19 silicate, 0.4 fluorides and TDS 197 in mg/L. (c) in 0.1 N HCl and 0.1 N NaOH at different time intervals from 2 to 24 h. In the leaching processes, each glass sample was placed in a 200 ml polyethylene BD Falcon TM conical tube with flip top cap, which allowed the leaching solution (150 ml) to completely cover the whole glass surfaces. The ratio of glass

Table 2 Chemical analysis of the prepared glasses in atomic %

Elements	O	Si	Na	Ti	Fe	Cu	Zn	Ca	Al	Total
G1	5.8	46.3	21.7	0.0	1.0	0.3	0.2	23.6	1.1	100.00
G2	2.3	43.2	9.8	0.3	3.3	–	–	40.4	0.7	100.00
G3	10.1	27.4	37.2	0.7	4.6	0.2	0.1	19.7	0.0	100.00

surface area to leachant volume (S/V) was kept at 1.87 $m^2 L^{-1}$ ± 0.1.

Scanning electron microscopy (SEM) model Jeol-JSM 5400 was used to study the surface morphology of the specimen at high magnifications before and after corrosion processes.

Density of each glass sample was measured three times with a maximum error 0.0002 g/cm^3 by using the suspended weight method based on Archimedes principle. Microhardness of each sample is also measured by using a Shimadzu microhardness tester after equal cutting and polishing of samples. The diamond -shaped indentation was measured with an estimated accuracy of ±0.5 μm testing with a load of 100 g at each 20 s. without causing visual micro cracks.

FTIR spectra of glasses were measured at room temperature at the wave number range 400–4000 cm^{-1} using spectrometer type VERTEX 70, FT/IR-430, Japan.

The EPR spectra of unirradiated and irradiated samples were recorded using EMX spectrometer (X-band), the cavity used was the standard Bruker ER 4102 rectangular cavity, Germany. The operating conditions for the EPR spectrometer were; microwave power 2.553 mW, modulation amplitude 9 G, time constant 81.92 ms and conversion time 20.48 ms. Samples were inserted in EPR tubes and measured at the above instrument parameters.

DSC measurements were used by using SHIMADZU DSC - 50 to determine the transition temperatures of the glass samples. The samples were heated from R.T. up to 700 °C with heating rate 10 deg./min. The reference substance was alumina powder of high purity and the temperature error was ±5 °C.

The gamma ray source used in irradiating glasses during the whole experimental work was Co^{60} gamma cell (2000 Ci) with a dose rate 1.338 kGy/ h at 30 °C. The glass samples were placed in the gamma cell in the manner that each sample was subjected to the same gamma dose.

3 Results

The municipal solid waste used in glass preparation was chemically analyzed by EDX technique after its burning at 700 °C. It is found that it contains the following elements: 13.25 O_2, 1.5 Na, 7.8 Al, 5.3 Si, 6.2 P, 47.1 Ca, 5.1 Fe, 2.5 K, 1.1 Cu, 1.2 Zn, 0.3 Ti, 3.2 S, 5.5 Cl, all in atomic% [7]. As it is obviously shown, the MSW contains glass forming oxides which enable it to be used as a raw material for the glass production after the addition of some amounts of glass forming oxides e.g. SiO_2 and B_2O_3 as shown in Table 1. Also, the differences in the concentration of elements between the three glasses shown in Table 2 may be due to the non-homogeneity of the taken sample from MSW during preparation of each glass. The studied physical and chemical properties are measured before and after both gamma irradiation and the in- situ corrosion in a solution of underground water where they represent alternative features for radiation emitted from the immobilized radioactive wastes and the water present under the earth, respectively. Or in other words, the surrounding environmental factors where the glasses are predicted to be exposed.

3.1 X- Ray Diffraction

X-ray diffraction spectra of the prepared glasses shown in Fig. 1 displays a broad hump with no sharp peaks detected for each glass composition. The spectra approve so that the amorphous structure of the prepared samples and their glassy natures.

3.2 Chemical Durability

Figure 2 shows the leaching process of the investigated glasses in a solution of underground H_2O solution at 90 - 100 °C for 16 h. It is observed from the figure that G3 with the higher content of Fe^{3+} is more durable than G1 and G2. Also, there is either decrease or relative stability in the weight loss percent of the glasses after exceeding 14 h.

Figure 3 shows the effect of in-situ corrosion in underground water at different gamma radiation doses where the leaching is relatively larger than that in Fig. 2. The prepared glasses show good durability with a relative stability in the weight loss percent until they reached to 200 kGy, a small increase is observed in their solubility.

Figure 4a, b shows the effect of HCl and NaOH solutions on the leaching process of the studied glasses, respectively. It

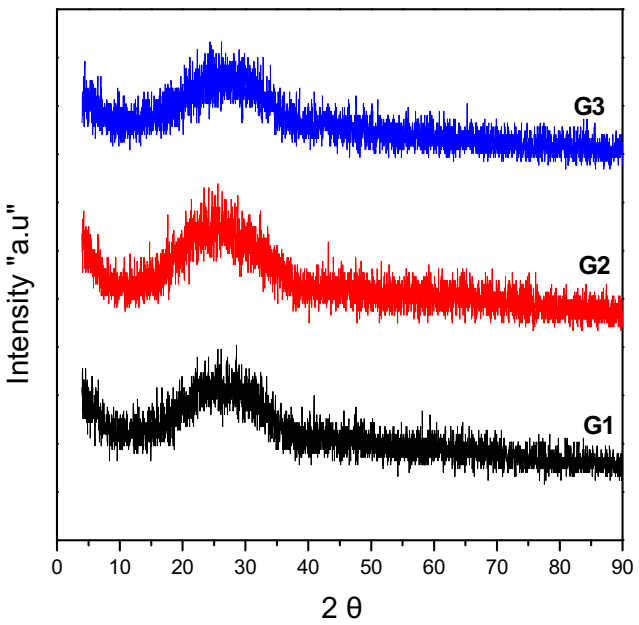

Fig. 1 XRD patterns of the prepared glasses

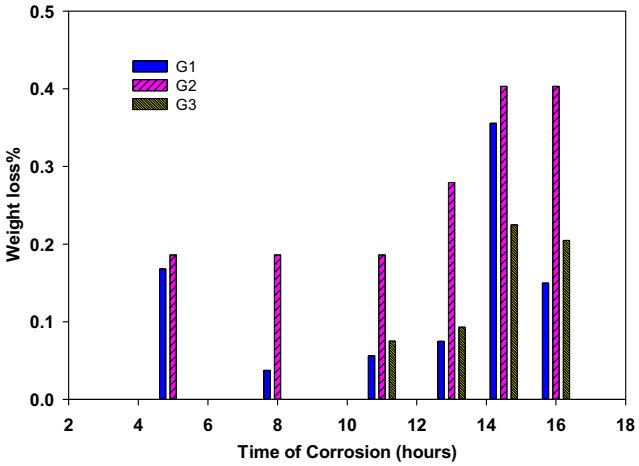

Fig. 2 Effect of underground H_2O solution on the weight loss% of glasses at different time intervals at 90 -100 °C

is observed that HCl is the highest corrosive solution and its leaching effect is greater than the effect of both underground H_2O and NaOH solutions.

3.3 Scanning Electron Microscopy SEM

Figure 5 shows SEM images of the glass surfaces before and after the in-situ corrosion in a solution of underground water at 200 kGy giving an agreement with corrosion results shown in Fig. 3.

3.4 Density and Microhardness

Density and microhardness results are shown in Table 3 where G3 has higher density but lower microhardness values than G1 and G2. The table shows also that there is a slight decrease in density and microhardness values of the prepared glasses under the effect of both corrosion and gamma radiation.

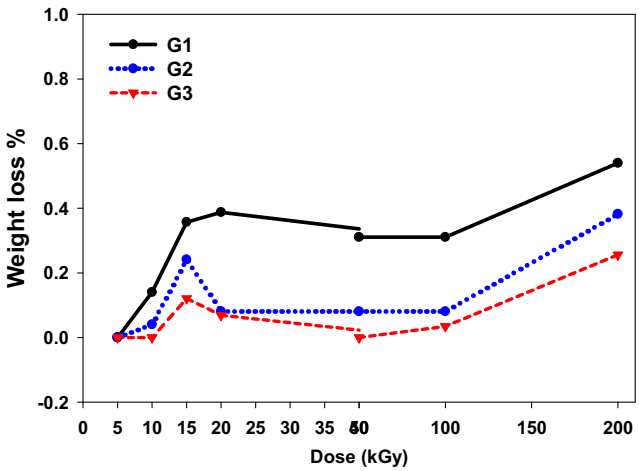

Fig. 3 Effect of underground H_2O solution on the weight loss% of glasses at different gamma irradiation doses

3.5 Infrared Absorption Spectra FTIR

The IR spectra obtained from the investigated glasses before irradiation is shown in Fig. 6. The overall IR spectral features of the prepared glasses are shown closely similar with few differences and they can be characterized by the appearance of the following bands;

(1) A small band at 400–600 cm^{-1}
(2) A sharp band at 680 cm^{-1} in the three investigated glasses
(3) Predominant high peaks at 920, 900 and 870 cm^{-1} for G1, G2 and G3 respectively.
(4) Medium bands at about 1350–1400 cm^{-1}
(5) Small bands at 2200 and 2350 cm^{-1} and 3700–3800 cm^{-1}

Figure 7 shows the effect of radiation on FTIR spectra on the three investigated glasses where there are slight changes between the spectra of glasses before and after gamma irradiation such as the appearance of a band at bout 1580–1730 cm^{-1}.

Figure 8 shows FTIR spectra of the prepared glasses before and after their in-situ corrosion in underground H_2O at 200 kGy of gamma radiation where there are some observed changes in the intensity and location of bands and sharpness of some bands due to the effect of both radiation and leaching such as;

(1) A sharp peak at about 1750 cm^{-1}
(2) A small shoulder at 1460 cm^{-1}
(3) A small peak at 1435 cm^{-1}
(4) A shoulder centered at about 1380 cm^{-1}
(5) A sharp peak at 1225 cm^{-1}
(6) A high peak at 980 cm^{-1} for G1
(7) A sharp band at 660–680 cm^{-1} and small peaks at 690 cm^{-1} or 540 cm^{-1}

3.6 Electron Paramagnetic Resonance Spectra EPR

It is observed from EPR spectra shown in Fig. 9 that the three glasses have relatively similar EPR intensities with good stability before and after the in-situ corrosion in underground H_2O at different gamma irradiation doses. It is observed also that G3 has the lowest and the more stable EPR intensities. There is also a common observation that the dose of 50 kGy gives the lowest EPR intensity in the three investigated glasses. It is also observed from the response curve shown in Fig. 10 that there is a good stability for each glass against different doses of gamma radiation. The figure shows

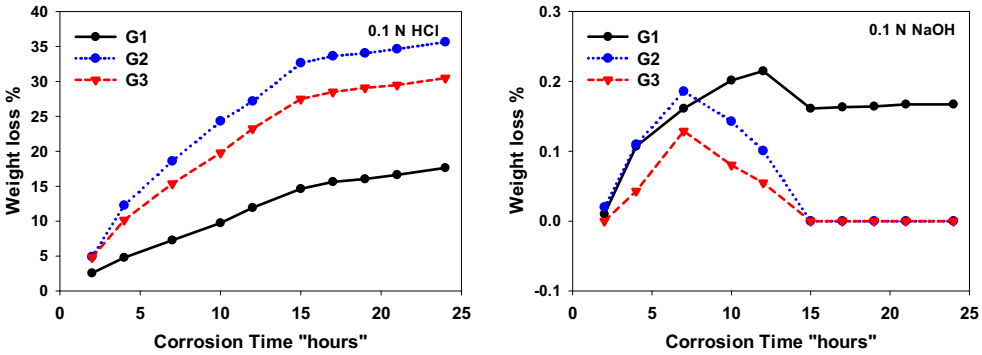

Fig. 4 Effect of **a** 0.1 N HCl and **b** 0.1 N NaOH solutions on the weight loss% of glasses at different time intervals

approximately straight lines of glasses spin numbers with the variation in radiation doses from 0 up to 200 kGy.

3.7 Differential Scanning Calorimetry DSC

Figure 11 shows the DSC curves of the three investigated glasses showing the values of glass transition temperatures of glasses "Tg" at about 350, 217 and 252 °C while the onset of crystallization temperature appear at about Tc = 550, 350 and 352 °C for G1, G2 and G3 respectively. However, melting temperatures (Tf) of glasses have not been recognized in the used temperature range.

4 Discussion

4.1 Chemical Durability

To predict the long-term behavior of high-level radioactive waste glass, it is necessary to study aqueous dissolution of the glass matrix under geological repository conditions [17]. Glass is generally considered to be a quite stable and relatively strong material but when it becomes in contact with water vapor or a liquid, it becomes to be affected [18]. The ability of glass surface to resist water and different chemical agents is called chemical durability. Chemical durability of glasses can be explained by two possible mechanisms, leaching and etching. (1) The ion-exchange leaching process takes place in acidic and dilute aqueous solution and it is deliberated to the release of mobile cations from the glass structure to the leaching solution or the replacement of alkali ions (M^+) with hydrogen or hydronium ions from the attacking solution forming of a leached layer, i.e. alkali depleted layer, according to the following reactions:

$$\equiv Si\text{–}O\text{–}M_{(glass)} + H^+{}_{(aq)} \rightarrow \equiv Si\text{–}O\text{–}H_{(glass)} + M^+{}_{(aq)} \quad (2)$$

$$= B\text{–}O\text{–}M_{(glass)} + H^+{}_{(aq)} \rightarrow = B\text{–}O\text{–}H_{(glass)} + M^+{}_{(aq)} \quad (3)$$

When the depleted layer becomes thicker, the diffusion rate of the mobile ions gradually slows down. (2) The etching or matrix dissolution mechanism that takes place in the alkali

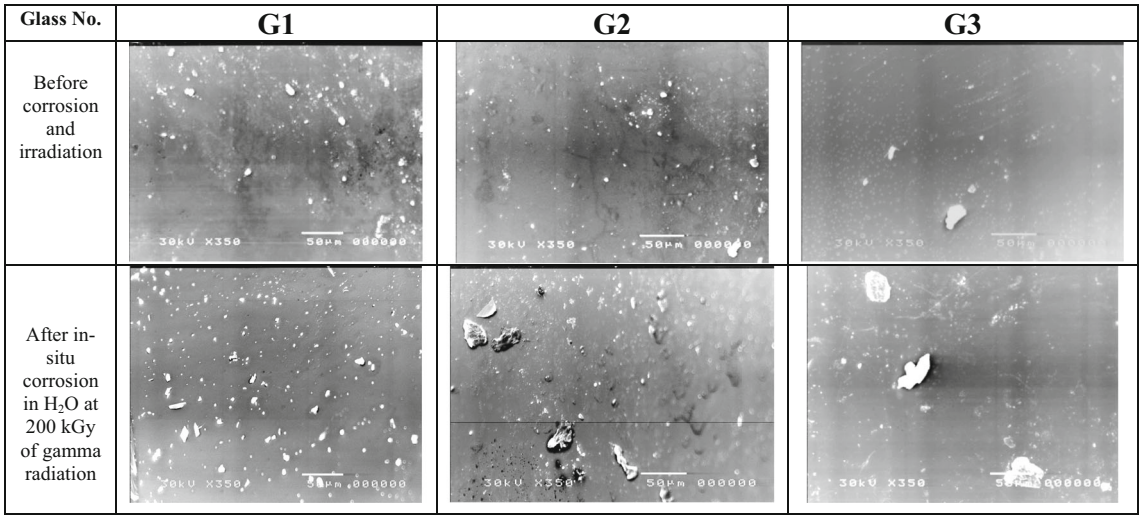

Fig. 5 SEM photographs of the prepared glasses before and after in-situ corrosion in H_2O at 200 kGy of gamma radiation

Table 3 Density and microhardness values before and after gamma radiation

Glass No.	Density before irradiation g/ cm^3	After irradiation situ 200 KGy	Microhardness before irradiation kg/mm^2	Microhardness after irradiation situ 200 KGy kg/mm^2
G1	2.6179	2.5883	553	548
G2	2.6447	2.6288	524	510
G3	2.6679	2.6599	504	502

media and it involves the dissolving of the glass network into the solution and breakdown of the total glass structure [19] according to the following reactions;

$$\equiv Si-O-Si\equiv_{(glass)+}\ 2OH^{-}_{(aq)} \rightarrow 2\equiv Si-OH_{(glass)} \quad (4)$$

$$=B–O–B=_{(glass)}+2OH^{-}_{(aq)} \rightarrow 2=B–OH_{(glass)} \quad (5)$$

Depending on the previous eqs. (2–5), it is relatively clear that the whole effect of the interaction between a glass structure and a solution is dictated by the rates at which the two mechanisms take place. Also, the concentration of the non-bridging oxygen atoms (NBO) and bridging oxygens atoms (BO) plays an essential role in determining the glass durability because H^+ exchanges with M^{n+} through the leaching mechanism however OH^- breaks the ≡Si-O-Si≡ and / or = B-O-B = linkages through the etching mechanism [19–21].

Therefore, the controlling factors affect leaching process depend on the concentration of BO_3, BO_4 and SiO_4 groups where the triangles BO_3 groups are more soluble than the tetrahedral BO_4 and SiO_4 groups. Since the later units are firmly attached in their four directions and with near alkali ions to neutralize the surplus of negatives charges.

4.1.1 Effect of Glass Composition on the Leaching Process

Corrosion of glasses depends on many factors such as glass composition, pH of the leaching solution, surface area, time, temperature as well as the transition times in between the ion exchange to hydrolysis. At high temperatures the time between the two processes is relatively short takes from hours to days however at low temperatures the ion exchange processes takes place rather than hydrolysis for tens to hundreds of years beforehand hydrolysis will be trivial in the total account of released cations [22]. So it is very important to study chemical durability of the investigated glasses at high temperatures depending on Bacon assumption [23] who concluded that, subjecting glasses to the effect of leaching solution around 100 °C for one hour, equals the action at room temperature for one year.

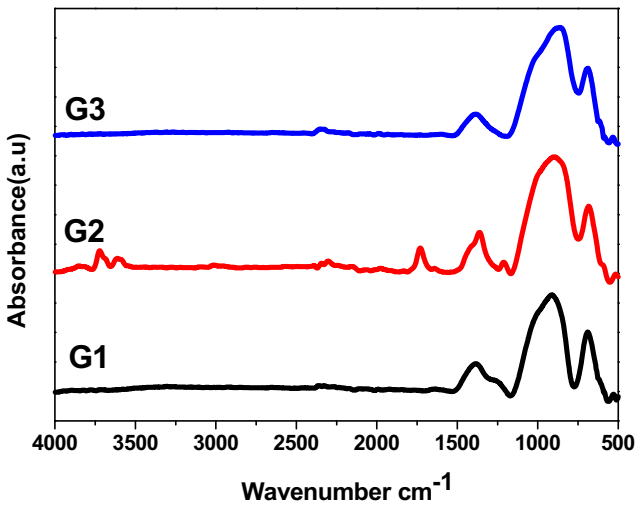

Fig. 6 FTIR spectra of investigated glasses before irradiation

Each metal oxide participated in the glassy network has its own effect on the durability of its glass and the combination of metal oxides in different concentrations acquires the glass its characteristic corrosion behavior. For instance; Na^+ ion is a network modifier and it can be present predominantly in the waste as shown in Table 1. Na^+ ions tend to increase the glass alterability by disrupting its structure through the creation of percolation channels that are defined by NBO at the ends of the highly ordered network regions, which ionically bond to alkalis [24]. Presence of small amounts of transition metals such as Cu^{2+}, Zn^{2+}, Ti^{4+} and Fe^{3+} were found to improve the chemical durability of glasses [14]. Ti^{4+} and Al^{3+} ions are intermediated oxides, they can act as network formers according to their contribution in the glass. Al^{3+} ions lengthen the glass by increasing its working range, and arise as AlO_4 strong tetrahedral structural units. While Ti^{4+} ions take up four-, five- or six-fold coordination in glasses. Ti^{4+} ions participate also as TiO_4 tetrahedral units in the glassy network. Both AlO_4 and TiO_4 units enhance the viscosity, stability and chemical resistance of their glasses [24]. Ca^{2+}, Mg^{2+} and Zn^{2+} ions improve the glass durability by stabilizing of the glass structure. Since, oxygen atoms that are bound to silicon/boron form the coordination polyhedral cells around these ions. In spite of that, volatility is increased with CaO, Na_2O or B_2O_3 addition, so that a technological compromise should be made depending on the composition of the used waste. Fe_2O_3 has two possible coordinations, 4 and 6 so it occupies a tetrahedral or an octahedral sites depending upon its content and the temperature e.g. in glasses contain $Fe_2O_3 < 4$ mol%, the tetrahedral sites are favored at high temperature. When the temperature of the glass containing Fe^{3+} is increased, the glassy structure is relaxed and changed from octahedral to tetrahedral iron

coordination, leading to a typical increase in the glass chemical durability [14]. The last assumption can discuss the high durability of G3 with the higher content of Fe^{3+} at the high temperature as shown in Fig. 2. Also, the relative stability in corrosion behaviors after exceeding 14 h may be related to the formation of insoluble hydrated layers that are deposited on the glass surface causing retardation of the leaching process or due to the formation of complex aluminum species [18].

4.1.2 Effect of Irradiation on Leaching Process

The relatively small increase in leaching behaviors of glasses at 200 kGy shown in Fig. 3 may be due to the penetration of protons or hydronium ions from H_2O solution to the glass structure that are facilitated by irradiation. Gamma radiation causes induced damage revealed by the presence of large vacancies and NBOs, therefore the chance for the formation of more free radicals and increasing the leaching rate may take place. It is obviously shown that corrosion behavior of G1 with irradiation is different from its behavior with temperature. This behavior can be discussed according to the assumption of Sheng et al. [25] who assumed that the solubility of various elements precipitated during the course of reaction is the controlling step in the leaching mechanism and the rate limiting step in the reaction is the removal of Si $(OH)_4$ groups from the glass surface. According to the last hypothesis it can be understood that G1 with the highest silica content (~ 46.3 atomic %) has the lowest durability with irradiation at 200 kGy.

4.1.3 Effect of Attacking Solution on the Leaching Process

The corrosion influence of HCl solution is greater than the effect of underground water as shown in Fig. 4a. Because of the known complete ionization of acids that provides higher quantities of H^+, H_3O^+ ions in contact with the glass surfaces, so higher leaching process is expected. The observed variations in corrosion process among the three studied borosilicate glasses can be related to the difference in their chemical compositions as shown in Table 2 [26]. Addition of sodium and/or boron to a silicate glass usually increases the dissolution rate. This is particularly true in acidic medium below pH 4 where the hydrolysis of Si-O-B bonds can be catalyzed by protons [27].

It is also obviously shown from Fig. 4a that G1 is more durable than G2 and G3 which can be understood by taking into consideration the chemical analysis of G1 glass surface composition shown in Table 2. G1 contains the highest percent of Si that forms the main tetrahedral super structural units SiO_4 and then strengthens the network structure. Also it contains relatively high content of Ca^{2+} ions (23.6 atomic %) that have large ionic radii and makes blocking in the diffusion routes of the released sodium ions causing a retarding in the leaching process. By comparing the durability of G1 and G3 in HCl with respect to their chemical analysis listed in Table 2,

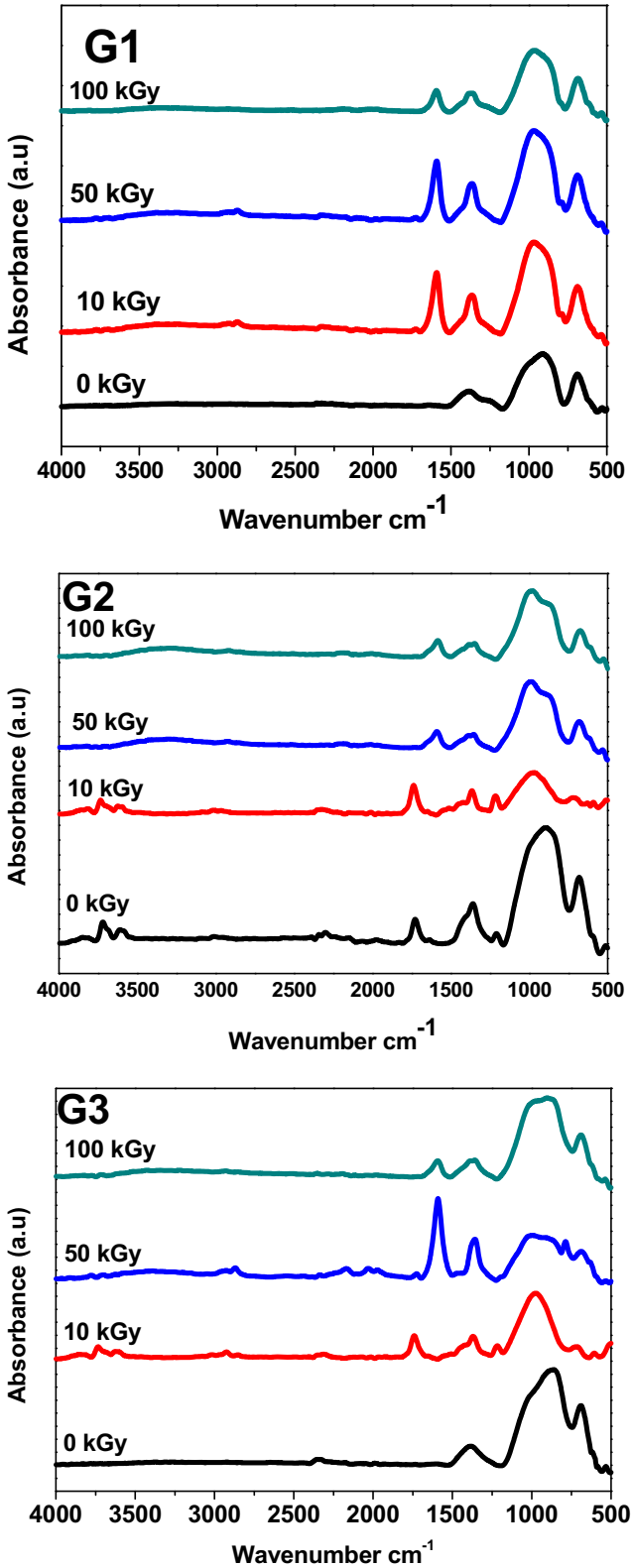

Fig. 7 FTIR spectra of the glasses before and after different gamma radiation doses

G1 has lower Na^+ content and it is known that the first step in the corrosion process is controlled by the release of mobile

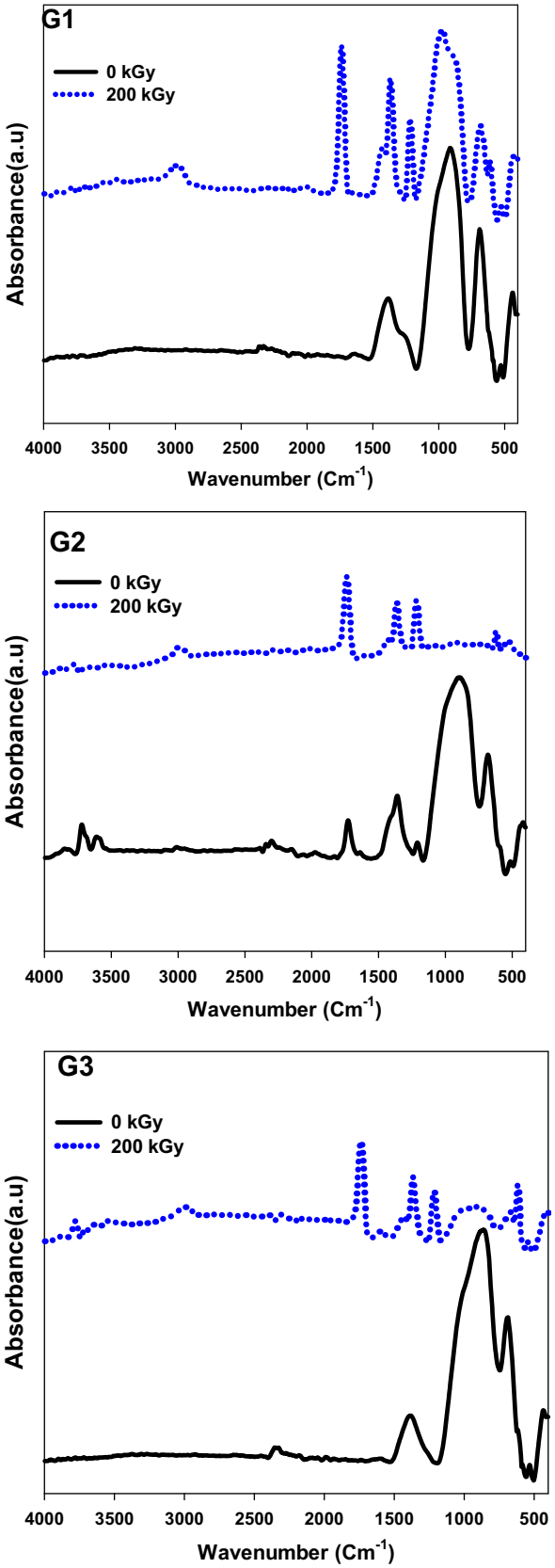

Fig. 8 FTIR spectra of the glasses after in-situ corrosion in underground water and irradiation with 200 kGy

sodium ions in the ion exchange process. Therefore there is a large deterioration in the glass durability with the increase of Na^{+} content like the case of G3. As well as contents of Al^{3+}, Cu^{2+} and Zn^{2+} ions are higher detected in G1 than G3 in which all of them increase the viscosity of the glass matrix and its durability. Also it was previously recorded that durability could be improved by increasing the silica or alumina content or by decreasing the amount of alkali oxide [9, 28].

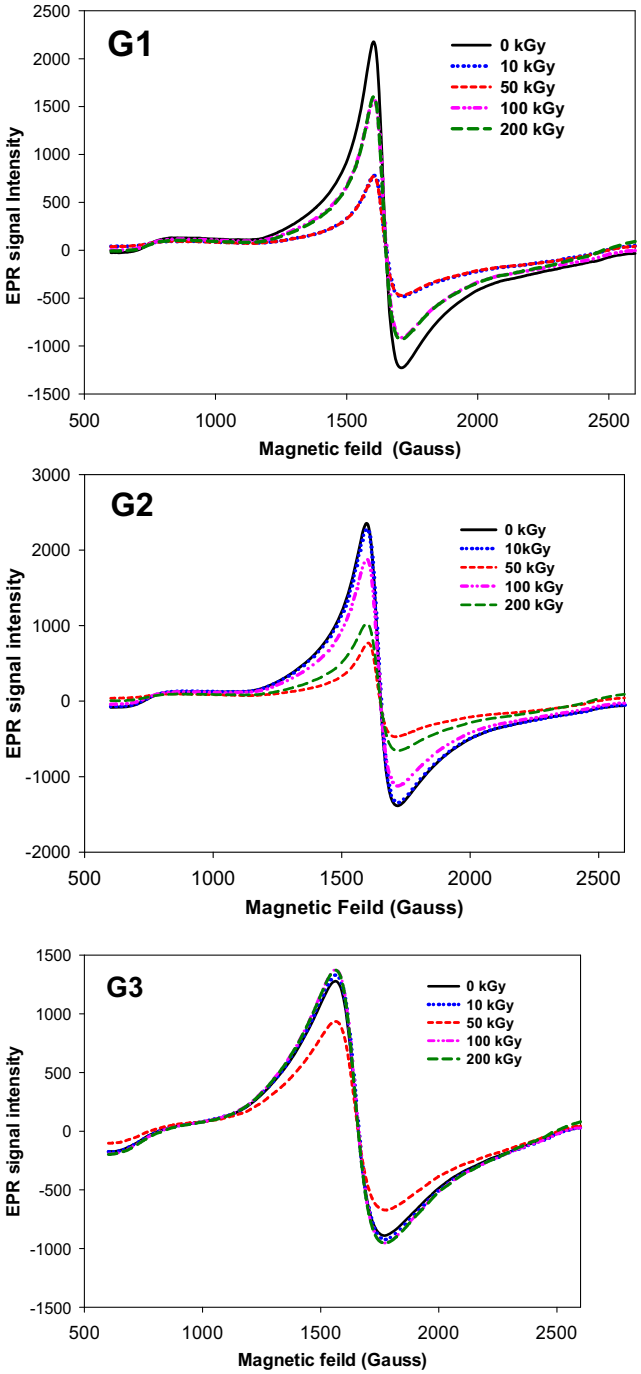

Fig. 9 EPR spectra of the three investigated glasses at different gamma radiation doses

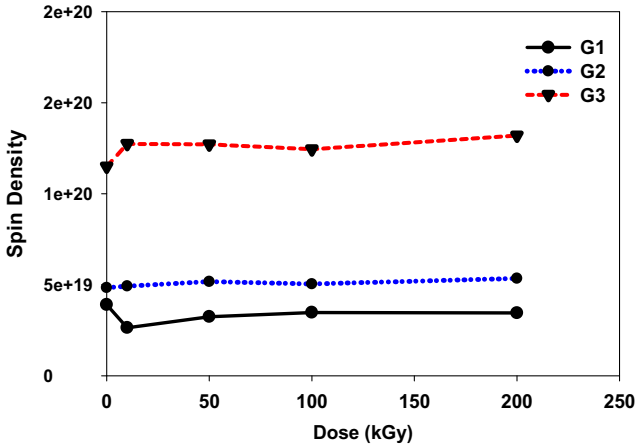

Fig. 10 Dose response curve of G1, G2 and G3 samples at different doses from 10 to 200 kGy

Therefore; G1 is the most durable in HCl solution. In spite of that, HCl represents the highest corrosive leaching medium and it is not preferred to use the investigated glasses in such acidic medium.

The effect of NaOH leaching solution is observed to be greatly less than the effect of acidic solution as shown in Fig. 4b. In basic solutions, network hydrolysis takes place where the bonds to borate groups can be hydrolyzed slightly faster than the silicate network depending on the glass composition, either immediate selective leaching of sodium and boron ions or the uniform glass dissolution. Glass dissolution of borosilicate glasses leads to the formation of silanol groups. Whether silanols are formed by Si-O-B bond hydrolysis or ion-exchange on non-bridging oxygens, they can repolymerize to

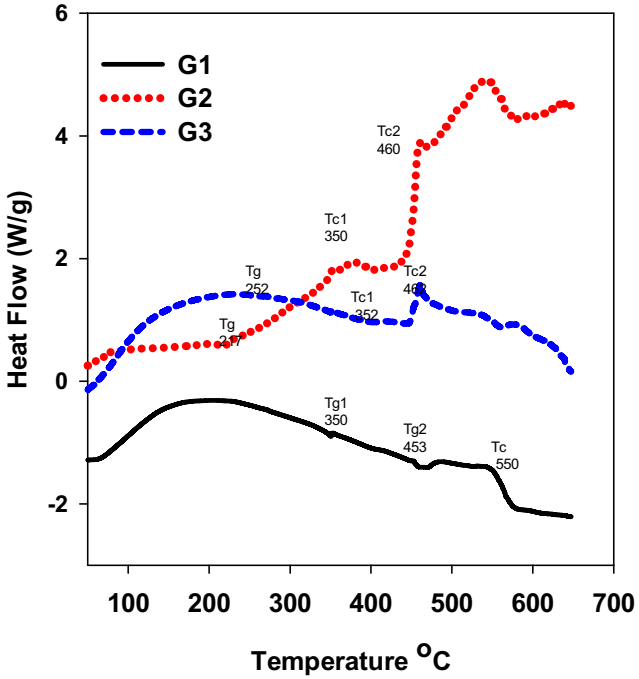

Fig. 11 DSC curves of the prepared glasses

produce 'colloidal silica' leached layers [29] or precipitate surface gelatinous hydroxides on the glass surface that retard the continuation of the leaching process [30]. This behavior discusses the high durability of glasses in NaOH solution and their stability at the end of corrosion. The results show also that G3 with the lowest Si content is the most durable which may be related to the removal of Si $(OH)_4$ groups according to the previous assumption of Sheng et al. [25].

4.2 Scanning Electron Microscopy SEM

SEM is studied to characterize glass surfaces morphology of the leached layers formed after corrosion processes where there is an agreement with corrosion results shown in Fig. 3 verifying the high chemical durability of the investigated glasses in H_2O solution. At the highest gamma radiation dose (200 kGy), the surfaces become slightly rough with non-uniformities due to the formation of some voids and precipitated layers since the leaching process involves hydrogen bearing ions and alkali ions leaves behind silica and /or boron rich layers containing hydrated micro pores [31].

4.3 Density and Microhardness

According to density results shown in Table 3, the prepared glasses have good and close density values however; G3 with higher Fe^{3+} content has higher density but lower microharness values than G1 and G2. Even though, all of them still have high and suitable density and microhardness values.

Density of glass is very important parameter that gives information about the structure of the glass besides the effect of various components in the glassy matrix, and how they firmly located in the glass network [32]. So every metal oxide contributes in the glass network would have its own influence on the density of its glass according to its characteristic properties and the way of interconnection with other glass constituents [12]. In borosilicate glasses where the two strong glass forming oxides B_2O_3 and SiO_2 form the network, B_2O_3 shares in the glassy network with the triangular BO_3 and tetrahedral BO_4 structural building units. However, SiO_2 shares with the tetrahedral $[SiO_4/2]^0$ units where the four oxygens in SiO_4 tetrahedral are participated. Introducing of metal oxides that may act as modifiers such as Na_2O, CaO, Al_2O_3 and Fe_2O_3 makes some disruption in borosilicate glassy network such as the depolymerization of Si–O–Si network that lead to the formation of meta, pyro and ortho-silicates [33]. As well as the conversion between triangular BO_3 and the tetrahedral BO_4 structural groups. Density is early defined as the weight per unit volume so it depends mainly on the masses of introduced ions that participated in the glass network. Consequently in most cases, the higher the atomic mass of the introduced ion, the expected higher density of its glass [34]. Therefore, G3 with higher Fe^{3+} content has the highest density values since

$Fe^{55.93}$ions has higher atomic mass than $Ca^{40.08}$ and $Al^{26.98}$ ions. Na^+ ions that have small ionic radii can fit itself easily in the interstices or vacancies present in the network and housing of Na^+ ions in the interstices leading in turn to the formation of more oxygens and more NBO [7]. Consequently gives high density values as it is obvious in Table 3 where G3 has the highest Na^+ ions content (~37.2 atomic %). On the other hand Ca^{2+} ions are present in high percentages in the investigated glasses as shown in their chemical analysis in Table 2. Such large divalent ions are strongly held in the interstices more than the monovalent Na^+ ions because the tetrahedral SiO_4 and BO_4 groups are more stable around the divalent ions than the monovalent ions. Ca^{2+}ions are in turn increases the compactness of the network and increase its density. According to the priority concept to divalent ions over monovalent ions, G2 with higher Ca^{2+} content has higher density than G1 with lower Ca^{2+} content regardless to their monovalent Na^+ ions concentrations [7].

Microhardness is an important mechanical parameter that is used to measure the strength of the glass and its ability to bear loads. Nuclear waste glasses should have high microhardness in order to achieve the intended purpose for radioactive immobilization. Microhardness values depend greatly on the glass composition and the introduced ions. Since glasses containing ions with large ionic radii and high polarizability should give lower microhardness values such as Fe^{3+} ions [35]. These large ions can act as potential barriers to the motion of groups and atoms thus increasing the polarizability of oxygen ions because the larger the ionic radii, the lower its ionic strength in the network. This in turn may lead to the formation of larger applied volume and lower microhardness values. Consequently, G3 with the higher Fe^{3+} content has lower microharness values than G1 and G2. Also Al^{3+} ions have an effective role in enhancing hardness of glasses so G1 that has slightly higher Al^{3+} ions content has the highest hardness values because it preferred to Al^{3+} ions to consume some of the available oxygens to give the four fold coordination AlO_4 instead of changing BO_3 to BO_4 [7]. In borosilicate system particularly, B takes part to form polymeric chains with Si, and then partially replacing the Al in its function and improves the connectivity of the structure in favor of a higher stable 3-D cross-linked network. This structure enhancement denotes therefore better mechanical properties [36].

4.3.1 Effect of Gamma Radiation on Density and Microhardness

In spite of the good stability of the glasses after their in- situ corrosion at 200 kGy, the slight decrease in density and microhardness values may be due to the possible atomic displacements that are caused by γ- collisions with the glass structure, which may significantly change stresses in the glass matrix [37]. As well as the recoiled oxygen ions from the glass that may give an explanation for the volume changes that is related directly to microhardness values. According to Arora et al. [38] the decrease in the density because of radiation is due to the creation of dangling bonds, NBOs, and creation of new bonds in the glass network that allow the structure to relax and fill the moderately large vacancies present in the interconnected glassy network of boron and oxygen atoms. In borosilicate glasses, the radiation creates displacements and electronic defects as well as weakens in Si–O–Si, B–O–B or Si–O–B bonds causing an interconversion of $BO_4 \rightarrow BO_3$ structural units and from ortho silicate units to pyro silicates therefore, the compactness of bulk density of the samples would be slightly decreased [12]. On the other side, when the corrosion process takes place at the high radiation dose like 200 kGy, it allows the etching process to take place through the hydrolysis mechanism and the network begins to breakdown causing an expansion of the volume and the exposed surface area, then both of density and microhardness values would be weakened.

4.4 Infrared Absorption Spectra FTIR

4.4.1 Effect of Composition on FTIR Spectra of the Investigated Glasses

FT-IR spectroscopy helps in the analysis of the environmental natures of different cations present in the glassy network and gives detailed information about the structural building units in which the glass consists of [39]. The features of the obtained spectral results shown in Fig. 6 indicate the predominance of vibrations of two main structural groups SiO_4, BO_3 and/ or BO_4 groups. The spectra shows overlapping between silicate and borate vibrations where the lack of peak sharpness may be related to the general disorder or non-periodic arrangement in the network, essentially because of the wide distribution of polymerization in the glass network representing the presence of bridging oxygen units in the glass. The observed overall IR spectral features of the prepared glasses can be interpreted as follows;

(1) The observed small peak appeared at 400–600 cm^{-1} may be related to the presence of transition metal ions (Cu^{2+}, Zn^{2+}, Ti^{4+}, Fe^{3+}…) in octahedral units or the vibrations of modifier cations such as Na^+, Ca^{2+} and Al^{3+}, where all of them are present in different amounts according to each glass composition shown in Table 2.
(2) The obvious sharp peak at 680 cm^{-1} in the three investigated glasses may be related to Si-O-Si and O-Si-O bending modes or oxygen bridges between two trigonal boron atoms bending vibrations of borate groups [40].
(3) The peak at about 860–920 cm^{-1} is assigned to the Si–O– NBO stretching vibration [12] or vibrations of tetrahedral tri-, tetra- and penta borate groups [40]. According to Stoch and Sroda [41], the content of sodium oxide is related to the content of the former oxide SiO_2 and they

concluded that, as the percent of Na^+ ions increases, the content of SiO_2 decreased so the amount of NBO increases. Therefore, the peak at 920 cm^{-1} becomes slightly with higher intensity for G3 than G1 and G2 with the lower Na^+ content as shown in Table 2. [40]. Also, the predominant high peaks at 920, 900 and 870 cm^{-1} for G1, G2 and G3 respectively are related to the order of increasing in SiO_4 content- see Table 2- because increasing in silica content may cause a shifting of bands to higher wave numbers.

(4) The medium peaks appear at about 1350–1400 cm^{-1} are correlated to vibrations of triangular BO_3 groups [40] or corresponded to the asymmetric stretching of B-O bond in $[BO_3]$ and $[BO_2O]^-$ [42].

(5) The small bands appear at 2200 and 2350 cm^{-1} and 3700–3800 cm^{-1} are related to hydrogen-bonded OH stretching vibrations [43] or the essential free OH stretching vibrations that are physically absorbed water. The last two peaks are more obvious in G2 because of the physically absorbed water and OH groups [31]. The general observation in Fig. 6 is that there is no major changes between the spectra of the three investigated glasses because the substitution of Na^+ by Ca^{2+}, Al^{3+} or Fe^{3+} ions giving no definite changes in the main super structural units of borate and silicate groups so the skeleton of the glassy network remains approximately constant [31].

4.4.2 Effect of Radiation on FTIR Spectra of the Investigated Glasses

Gamma irradiation causes some alterations in FITR spectra of glasses [44] due to the possible changes in bond angles and/or bond lengths of the building groups in the glasses. Some mechanisms are proposed to explain variations on the IR spectra because of the effect of radiation, one of them is the displacement of lattice atoms or electron defects caused by radiation, which include changes in the valence states of lattice or impurity atoms [45]. Thus, the glass network and groups arrangement become more asymmetrical, leading to a weakening of the network grouping vibrations and changes in the average bridging bond angles. Effect of radiation on glass depends strongly on the glass matrix, its dopants and impurity as well as the type and energy of radiation and the total dose [46].

According to Fig. 7, there is a small effect of radiation on the investigated glasses since the only variation after irradiation was the appearance of the band at bout 1580–1730 cm^{-1} that may be related to the small concentration of NBO formed due to irradiation and it may be correlated to the asymmetric stretching relaxation of B-O bond of trigonal BO_3 units with NBO [12] or sometimes attributed to molecular water vibrations at 1640 cm^{-1} [38]. What is worth to mention is that, the vibrational modes of the main building groups remain unchanged in their numbers and positions, so the net result would be a nearby stability of the combined structural units with relatively similar FITR spectra before and after irradiation.

4.4.3 Effect of Leaching and Radiation

The observed changes in FTIR spectra of glasses before and after in-situ corrosion and radiation as shown in Fig. 8 are due to the selective alkali leaching of introduced modifier ions that causes the appearance of NBO band convolving e.g. they may troll together with the stretching bridging oxygens. The bending vibrations of the bridging oxygens become more intense and usually the stretching modes are more sensitive to structural changes than bending modes [46].

The small peaks at 2960–3025 and 3700–3800 represent hydroxyl groups, molecular water, hydrogen bonding or stretching peaks of = B-OH or ≡ Si-OH groups because of the penetration of hydrogen or hydronium ion into the glass matrix and water molecules that are typically associated with BO_4 and/or SiO_4 in the glass surface during the leaching process [18]. Primak [47] has explained early that radiation causes compaction in the glass by the decrease of bond angles of the building units such as Si-O-Si, B-O-B or Si-O-B that may explain the higher intensities of IR bands and the observed peaks at 500–1600 cm^{-1} due to the effect of radiation as shown in Fig. 8. It is known that irradiating glasses with gamma rays may yield displacement, bond breaking or knock-on destruction by electron rearrangement or radiolysis [48]. Such induced defects are thought to be momentary in their natures. Perera and Doremus [49] have been showed also that irradiation of an alkali containing glass outcomes in hole trapping thru the non-bridging oxygen, with one alkali ion trapping. Therefore, variations in the absorption bands in the borosilicate glasses may be due to several reasons; (a) oxygen atom in the network structure Si–O–Si or B–O–B configurations; (b) oxygen atoms in the intermediate, e.g., Si–O–Na or B–O–Na configurations (c) oxygen atom in neighborhood to a modifier, e.g., Si–O–Na and B–O–Na configurations [50].

From the spectra shown in Fig. 8, it is observed that the intensity of peaks in G1 at about 800–1200 cm^{-1} that are concerned to BO_4 groups is higher than the intensity of peaks at 1600–1200 cm^{-1}that are concerned to BO_3 units [51] because of the higher concentration of NBO in G1. Therefore a high peak at about 1750 cm^{-1} is appeared on G1 IR spectra as shown in Fig. 8 which is related to –OH groups reflecting its higher leaching behavior as shown in Fig. 3. This behavior can be also demonstrated by density results shown in Table 3. Since, the more blocked and denser structure delays the leaching mechanism because the strong glassy network with low NBO, retards the penetration of hydrogen or hydronium ions from the solution to the glass surface, and vice versa.

Figure 8 shows also the sharpness of the following bands due to the effect of both radiation and leaching; (a) A sharp peak at about 1750 cm^{-1} that may be related to the formation of water vapor after the fracture of the -OH bond due to the ion exchanging process according to De Aza et al. [52]. (b) The absorption band near 1430 cm^{-1} can be assigned to the stretch modes of the B–O–B bonds in $[BO_3]^-$ triangle in different borate groups [53] (c) A shoulder centered at about 1380 cm^{-1} corresponds to the asymmetric stretching of B–O bond in $[BO_3]$ and $[BO_2O]^-$ [42]. (d) A sharp peak at 1225 cm^{-1} related to pyro- and ortho borate groups. (e) The high peak appeared at 980 cm^{-1} for G1 originates from the symmetric stretching vibration of the Si–O–Si bond and the vibration of the Si–O terminal bond [53]. (f) A sharp band at 660–680 cm^{-1} due to bending vibrations of Si–O–B bridges [54] and small peak at 690 cm^{-1} or 540 cm^{-1} due to the isolated or condensed of AlO_4 tetrahedral groups respectively. So the peak position of AlO_4 groups is very close to that of SiO_4 and BO_4 groups thus, there are composite bands due to the combing of $[AlO_4]$ and $[BO_4]$ group vibrations [55].

4.5 Electron Paramagnetic Resonance EPR

EPR spectroscopy is an essential technique used to study the irradiation-induced transformations concerning paramagnetic defects, i.e. centers with unpaired electrons. Actually, the signals detected in the EPR spectra are deliberated as fingerprint of paramagnetic centers; they could give information on natures and kinetics of the structural changes taking place at the sites of these defects in both the amorphous and crystalline silica matrix [56].

Figure 9 shows the good stability and the similar EPR spectra of the studied glasses however, G3 has the most stable EPR intensities. This effect may be related to its density results since G3 has the highest density values where molecules are very close together giving more blocked and compact structure. Therefore the chance for passing photons declined and the photons loss their energies throughout the molecules without a variation in the chemical structure of the glass matrix reflecting the glass stability against different doses of radiation. It is observed also that the dose of 50 kGy gives the lowest EPR intensity which may be due to one of the following reasons;

(a) The production of some glass defects (i.e Si- E` and/or B- E` centers) is a two- step process, i.e. the low irradiation dose changes NBOHCs into intermediate configurations which are then converted into E`centers by increasing irradiation doses [57]. (b) The weak irradiation effect on the EPR intensity observed at early irradiation doses can be related also to the pertinent radiation levels which are too small to generate new vacancies. However, increasing radiation doses to 100 or 200 kGy causes the generation of new vacancies. (c) The presence of high concentration of H_2O molecules as shown in IR figures at 50 KGy may retard the existing of unpaired electrons and paramagnetic defect centers leading to a relatively lower EPR intensity.

The relative straight lines noticed in response curves of glasses as shown in Fig. 10, demonstrate the electronic stable behavior of glasses towards gamma radiation and the possibility to use the studied glasses as candidate for radiation shielding purposes or as nuclear waste glasses. The relative stability takes place at higher irradiation doses (100& 200 kGy) may be also related to the generation mechanism that overcomes the destruction process when the amplitude of the EPR spectra from defect centers come up to a saturated level [58]. The response curve shows also that G3 has higher spin density than G1 and G2 glasses. In my point of view, it may be due to the continuous conversion between the two valence states of iron $Fe^{2+} \leftrightarrow Fe^{3+}$ during the irradiation process that may lead to unrestricted conversion between the two spin states and then higher spin density. On the other hand G1 gives the lowest spin density reflecting the strong structure of its glass matrix.

4.6 Differential Scanning Calorimetry DSC

Differential scanning calorimetry (DSC) is an analytical technique that can provide information about thermal stability, and the structural conformation by measuring the thermal transition temperatures Tg, Tc and T_m. Well-defined endothermic and exothermic peaks at glass transition and crystallization temperatures were obtained by DSC curves shown in Fig. 11. The glass transition temperature represents the strength or rigidity of the glassy structure so there is a direct relation between the glass transition temperature T_g and glass composition where the most thermally stable glass has the highest glass-forming ability [59]. Thermal stability of glasses can be expected also by the calculation of temperature differences $T_c – T_g$ [60] from the results of Tg and TC in Fig. 11, G1 can be expected to has the highest thermal stability and G2 comes in the second order followed by G3 in the third order. The delaying of appearance of melting temperature of the three glasses in the used temperature range indicates also their good thermal stability.

5 Conclusion

Nuclear waste glass is one of the most important common applications of vitrification process and it depends mainly on borosilicate structure with two main structural groups of tetrahedral SiO_4 and triangular BO_3 or tetrahedral BO_4 groups. The contribution of these groups in the glassy network is responsible for acquiring glasses their characteristic properties before and after the in-situ corrosion in underground water and irradiation up to 200 kGy. Studying chemical durability of glasses shows their good stability in underground H_2O at

90-100 °C especially G3 with the highest Fe^{3+} content that gives high stability because of relaxation of its structure and conversion from octahedral to tetrahedral iron coordination. HCl is a highly corrosive leaching solution for the investigated glasses however; G1 gives the highest durability in it. G1 has high Si^{4+} and Ca^{2+} contents which strengthen its glass structure, lower Na^{+} content that is responsible for the large deterioration in the glass durability as well as suitable amounts of Al^{3+}, Cu^{2+} and Zn^{2+} ions that increase the viscosity of the glass matrix and its durability. The glasses show also high durability in NaOH solution and their stable behavior at the end of corrosion may be due to the precipitation of gelatinous hydroxides on the glass surfaces which retard the progress of the corrosion process. The prepared nuclear waste glasses have also good density and microhardness values where density is enhanced by the high molecular weight of Fe^{3+} and creation of NBO, due to fitting of Na^{+} ions into the interstices of the glass matrix. However microhardness is enhanced by the percent of Ca^{2+} and Al^{3+} ions, where the latter ions work to consume some of the available oxygens and form the four fold coordination AlO_4 rather than changing BO_3 to BO_4. The FTIR spectra show lack of peak sharpness because of the general disorder or non-periodic arrangement in the borosilicate network and due to overlapping between silicate and borate vibrations. Relatively stable IR spectra are detected where bands at 500–1600 cm^{-1} can be related to the concentration of BO_3 and BO_4 units however, bands at about 1600–4000 cm^{-1} may be concerned to the formation of either = B-OH or ≡ Si-OH groups because of the penetration of hydrogen ions into the glass matrix during the corrosion process. EPR spectra of the investigated glasses show relatively similar and low EPR intensities and their response curves give approximately straight lines which reflect the stable behavior of glasses towards gamma radiation doses. Tg and Tc values produced from DSC curves show also the good thermal stability of the investigated glasses. According to the present study, the prepared glasses give good and suitable properties to be used for the immobilization of high level radioactive wastes HLW especially in the neutral and alkaline solution, but it is not favorable to use them in an acidic medium.

References

1. Alexander K, Mario P, Alessandro H (2003) Sintered glass-ceramics from municipal solid waste-incinerator fly ashes-part I: the influence of the heating rate of the heating rate on the sinter-crystallization. Eur Ceram Soc 23:827–832
2. Yang J, Bo X, Boccaccini AR (2009) Preparation of low melting temperature glass–ceramics from municipal waste incineration fly ash. Fuel 88:1275–1280
3. Barbieri L, Bonamartini AC, Lancellotti I (2000) Alkaline and alkaline-earth silicate glasses and glass-ceramics from municipal and industrial wastes. Eur Ceram Soc 20:2477–2483
4. Maximina R, Jes´us VM (1999) Surface and bulk crystallization of glass-ceramic in the Na_2O-CaO-ZnO-PbO-Fe_2O_3-Al_2O_3-SiO_2 system derived from a goethite waste. Am Ceram Soc 82: 1313–1317
5. Vernaz E, Veyer C, Gin S (2016) Waste glasses. Elsevier, France
6. Baydogan N, Tugrul AB (2012) Borosilicate glass for gamma irradiation fields. Solid State Sci 14:1692–1697
7. El-Alaily NA, Abou-Hussein EM, Abdel-Monem YK, Abd Elaziz TD, Ezz-Eldin FM (2014) Vitrified municipal waste as a host form for high-level nuclear waste. Radioanal Nucl Chem 299:65–73
8. Roth G, Weisenburger S (2000) Vitrification of high-level liquid waste: glass chemistry, process chemistry and process technology. Nucl Eng Des 202:197–207
9. Donald IW, Metcalfe BL, Taylor RNJ (1997) Review: the immobilization of high level radioactive waste using ceramics and glasses. Mater Sci 32:5851–5887
10. Compton KL, Bennert DM, Bickford DF (1993) Regulatory issues in vitrification research: a case study of circuit board reclamation. Am Ceram Soc 39:3–12
11. Festa D, Gudagnino M (1995). Rivista della Stazione Sperimentale del Vetro 5:89–93
12. Rupesh Kumar A, Rao TGVM, Neeraja K, Rami Reddy M, Veeraiah N (2013) Gamma ray induced changes on vibrational spectroscopic properties of strontium alumino-borosilicate glasses. Vib Spectrosc 69:49–56
13. Kim M, Heo J (2015) Calcium-borosilicate glass-ceramics waste forms to immobilize rare-earth oxide wastes from pyro-processing. Nucl Mater 467:224–228
14. Azooz MA, El Batal HA, Abd El Moneim M (2005) Corrosion Behaviour of Some Gamma-Irradiated Phosphate Glasses for Radioactive Wastes Burial Applications. Trans Indian Ceram Soc 64:95–100
15. Vance ER, Begg BD, Gregg DJ (2017) Immobilization of high-level radioactive waste and used nuclear fuel for safe disposal in geological repository systems. In: Woodhead Publishing Series in Energy (2nd eds) Geological Repository Systems for Safe Disposal of Spent Nuclear Fuels and Radioactive Waste. Lucas Heights, NSW, Australia
16. Weber WJ, Ewing RC, Angel CA, Arnold GW, Cormack AN, Delaye JM, Griscom DL, Hobbs LW, Navrotsky A, Price DL, Stoneham AM, Weinberg MC (1997) Radiation Effects in Glasses Used for Immobilization of High-level Waste and Plutonium Disposition. Mater Res 12:1948–1978
17. De Echave T, Tribet M, Jollivet P, Marques C, Gin S, Jégou C (2018) Effect of clayey groundwater on the dissolution rate of SON68 simulated nuclear waste glass at 70 °C. Nucl Mater 503: 279–289
18. Ezz-Eldin FM, Abd-Elaziz TD, Elalaily NA (2010) Effect of dilute HF solutions on chemical, optical, and mechanical properties of soda–lime–silica glass. Mater Sci 45:5937–5949
19. Clark DE, Pantano CG, Hench LL (1979) Corrosion of glass. Books for industry, New York
20. Rana MA, Douglas R (1961) The reaction between glass and water. Part 1. Phys Chem Glasses 2:179–195
21. Rana MA, Douglas R (1961) The reaction between glass and water. Part 2. Phys Chem Glasses 2:196–204
22. Ojovan MI, Pankov A, WE Lee (2006) The ion exchange phase in corrosion of nuclear waste glasses. Nucl Mater 358:57–68
23. Bacon FR (1968) The chemical durability of silicate glass. The Glass Ind 49:442–449

24. Ojovan MI, Lee WE (2005) Immobilization of Radioactive Wastes in Glass. In: Elsevier Science (eds) An introduction to nuclear waste immobilization. Elsevier, Amesterdam
25. Sheng J, Luo S, Tang B (1999) The leaching behavior of borate waste glass SL-1. Waste Manag 19:401–407
26. El batal HA, Azooz MA, Saad EA, Ezz ELDin FM, Amin MS (2018) Corrosion behavior mechanism of borosilicate glasses towards different leaching solutions evaluated by the grain method and FTIR spectral analysis before and after gamma irradiation. Silicon 10:1139–1149
27. Bunker BC, Arnold GW, Day DE, Bray PJ (1986) The effect of molecular structure on borosilicate glass leaching. Non-Cryst Solids 87:226–253
28. Chick LA, Piepel GF, Mellinger GB, May RP, Gray WJ, Buckwalter CQ (1981) Battelle Pacific northwest labs., Richland, WA (USA) https://doi.org/10.2172/6270428
29. Bunker BC (1994) Molecular mechanisms for corrosion of silica and silicate glasses. Non-Cryst Solids 179:300–308
30. El Badry KM, Moustafa FA, Moenis AA, El Batal FH (2002) Corrosion behavior of some selected bioglasses by different aqueous solutions. Glass Technol Eur Glass Sci Tech Part A 43:162–170
31. El-Alaily NA, Abd-Elaziz TD, Soliman L (2015) Effect of iron slag on the corrosion resistance of soda lime silicate glass. Silicon 10: 11–20
32. Marzouk MA (2012) Optical characterization of some rare earth ions doped bismuth borate glasses and effect of gamma irradiation. Mol Struct 1019:80–90
33. Rao KJ (2002) Structural chemistry of glasses. Elsevier, Amsterdam
34. Abou Hussein EM, El-Alaily NA (2018) Study on the Effect of Gamma Radiation on Some Spectroscopic and Electrical Properties of Lithium Borate Glasses. Inorg Organomet Polym 28:1214–1225
35. Rachkovskaya GE, Zakharevich GB (2004) Properties, Structure, and Application of Low-Melting Lead–Bismuth Glasses. Glas Ceram 61:9–12
36. Taveri G, Tousek J, Bernardo E, Toniolo N, Boccaccini AR, Dlouhy I (2017) Proving the role of boron in the structure of fly-ash/borosilicate glass based geopolymers. Mater Letters 200:105–108
37. Ezz El-Din FM, El Alaily NA, El-Batal HA (1992) Density and refractive index of some γ-irradiated alkali silicate glasses. Radioanal Nucl Chem 163:267–275
38. Arora M, Baccaro S, Sharma G, Singh DP (2009) Radiation effects on PbO–Al2O3–B2O3–SiO2 glasses by FTIR spectroscopy. Nucl Instrum Methods Phys Res B 267:817–820
39. Abdelghany AM, ElBatal HA (2014) Gamma-rays interactions on optical, FTIR absorption and ESR spectra of 3d transition metals-doped sodium silicophosphate glasses. Mol Struct 1067:138–146
40. Abdelghany AM, El-Damrawi G, Oraby AH, Madshal MA (2018) Optical and FTIR structural studies on CoO-doped strontium phosphate glasses. Non-Cryst Solids 499:153–158
41. Stoch L, Środa M (1999) Infrared spectroscopy investigation of oxide glasses structure. Mol Struct 511–512:77–84
42. Nattapol L, Panida P, Pinit K, Phetlada K, Weerinradah T, Ratchadaporn P (2016) Boron and pentavalent vanadium local environments in binary vanadium borate glasses. Non-Cryst Solids 453:118–124
43. Dunken H, Doremus RH (1987) Short time reactions of a Na2O-CaO-SiO2 glass with water and salt solutions. Non-Cryst Solids 92:61–72
44. El-Batal FH (2004) Gamma rays interaction with some sodium borate glasses containing MoO_3. Egypt J Chem 47:101–126
45. Sharma G, Singh K, Manupriya MS, Singh H, Narang SB (2006) Effect of gamma irradiation on optical and physical properties of $PbO–Bi_2O_3–B_2O_3$ glasses. Radiat Phys Chem 75:959–966
46. Manupriya K, Thind S, Sharma G, Singh K (2007) Soluble borate glasses: in vitro analysis. Amer Ceram Soc 90:467–471
47. Primak W (1972) Mechanism for the Radiation Compaction of Vitreous Silica. Appl Phys 43:2745–2754
48. Ahmed AA, Abbas AF, Youssof IM (1995) Attack of lead crystal glass by aqueous solution of ethyl and methyl alcohol: proceedings XVII International Congress on glass. Chinese Ceram Soc 3:239–244
49. Perera G, Doremus R (1991) Dissolution Rates of Silicate Glasses in Water at pH 7. Am Ceram Soc 74:1269–1274
50. Jincheng D, Cormack AN (2005) The structure of erbium doped sodium silicate glasses. Non-Cryst Solid 351:2263–2276
51. Ashok B, Kumar RV, Kistaiah P (2015) Effect of alkaline earths on spectroscopic and structural properties of Cu^2+ ions-doped lithium borate glasses. Non-Cryst Solids 426:47–54
52. De Aza AH, Turrillas X, Rodriguez MA, Duran T, Pena P (2014) Time-resolved powder neutron diffraction study of the phase transformation sequence of kaolinite to mullite. Eur Ceram Soc 34: 1409–1421
53. Hua Gui, Cui Li, Changwei Lin, Qian Zhang, ZhiweiLuo, Lei Han, Jianlei Liu, Taoyong Liu, Anxian Lu (2018) Glass forming, crystallization, and physical properties of $MgO-Al_2O_3-SiO_2-B_2O_3$ glass-ceramics modified by ZnO replacing MgO. Eur Ceram. https://doi.org/10.1016/j.jeurceramsoc.2018.10.002
54. El-Egili K (2003) Infrared studies of $Na_2O-B_2O_3-Si_2O$ and $A1_2O_3$; Na_2O - B_2O_3- Si_2O glasses. Physica B 325:340–348
55. El Batal FH, Ashour AH (2003) Effect of gamma irradiation on the electrical conductivity of ternary borate glasses. J Mater Chem Phys 77:677–686
56. Alessi A, Girard S, Cannas M, Agnello S, Boukenter A, OuerdaneY (2012) Influence of drawing conditions on the properties andradiation sensitivities of pure-silica-core optical fibers. J Light Technol 30:1726–1732
57. Agnello S, Boscaino R, Canas M, Gelardi FM (2000) Creation of paramagnetic defects by gamma irradiation in amorphous silica. Appl Magn Res 19:579–585
58. Mahmud HH, Mansour A, Ezz-Eldin FM (2014) Generation and bleaching of E′-centers induced in a-SiO_2 by γ-irradiation. Radioanal Nucl Chem 302:261–272
59. N'Dri K, Sei J, Houphouet-Boigny D, Kra G, Jumas JC (2007) Estimation of glass-forming ability and glass stability of Sb_2S_3-As_2S_3-Sb_2Te_3 glasses by thermal properties. Appl Sci 7:3167–3176
60. Jain PK, Deepika, Saxena NS (2009) Glass transition, thermal stability and glass-forming ability of Se90In10-xSbx (x = 0, 2, 4, 6, 8, 10) chalcogenide glasses. Philos Mag 89:641–650